

UNCLASSIFIED

Defense Technical Information Center
Compilation Part Notice

ADP011217

TITLE: Development of 200-Channel Mapping System for Tissue Oxygenation Measured by Near-Infrared Spectroscopy

DISTRIBUTION: Approved for public release, distribution unlimited

This paper is part of the following report:

TITLE: Optical Sensing, Imaging and Manipulation for Biological and Biomedical Applications Held in Taipei, Taiwan on 26-27 July 2000. Proceedings

To order the complete compilation report, use: ADA398019

The component part is provided here to allow users access to individually authored sections of proceedings, annals, symposia, etc. However, the component should be considered within the context of the overall compilation report and not as a stand-alone technical report.

The following component part numbers comprise the compilation report:

ADP011212 thru ADP011255

UNCLASSIFIED

Development of 200-channel mapping system for tissue oxygenation measured by near-infrared spectroscopy

Masatsugu Niwayama*, Daisuke Kohata, Jun Shao, Nobuki Kudo, Takafumi Hamaoka^a,
Toshihito Katsumura^a, and Katsuyuki Yamamoto

Division of Biomedical Systems Engineering, Graduate School of Engineering,
Hokkaido Univ., Sapporo 060-8628, Japan

^aTokyo Medical College, Shinjuku 6-1-1, Tokyo 160-8402, Japan

ABSTRACT

Near-infrared spectroscopy (NIRS) is a very useful technique for noninvasive measurement of tissue oxygenation. Among various methods of NIRS, continuous wave near-infrared spectroscopy (CW-NIRS) is especially suitable for real-time measurement and for practical use. CW-NIRS has recently been applied to *in vivo* reflectance imaging of muscle oxygenation and brain activity. However, conventional mapping systems do not have a sufficient mapping area at present. Moreover, they do not enable quantitative measurement of tissue oxygenation because conventional NIRS is based on the inappropriate assumption that tissue is homogeneous. In this study, we developed a 200-channel mapping system that enables measurement of changes in oxygenation and blood volume and that covers a wider area (30 cm x 20 cm) than do conventional systems. The spatial resolution (source-detector separation) of this system is 15 mm. As for the effects of tissue inhomogeneity on muscle oxygenation measurement, subcutaneous adipose tissue greatly reduces measurement sensitivity. Therefore, we also used a correction method for the influence of the subcutaneous fat layer so that we could obtain quantitative changes in concentrations of oxy- and deoxy-hemoglobin. We conducted exercise tests and measured the changes in hemoglobin concentration in the thigh using the new system. The working muscles in the exercises could be imaged, and the heterogeneity of the muscles was shown. These results demonstrated the new 200-channel mapping system enables observation of the distribution of muscle metabolism and localization of muscle function.

Keywords: near-infrared spectroscopy, tissue oxygenation, skeletal muscle, functional imaging

1. INTRODUCTION

Near-infrared spectroscopy (NIRS) has been applied to clinical measurements as a very useful technique for noninvasive measurement of tissue oxygenation. Tissue oxygenation is closely related to metabolic activity or the presence of disease. Chance¹ and co-workers first applied NIRS to imaging of metabolic activity of the brain. Maki *et al.*² developed optical topography, based on continuous wave spectroscopy (CW-NIRS) as a practical imaging method for observing brain activity. Cerebral oxygenation imaging using NIRS has recently been clinically applied to investigations of brain function^{3,4}. Several studies on muscle oxygenation imaging have also been carried out. Maris *et al.*⁵ obtained images of the forearm muscle using a mechanical scanning system consisting of several optical probes based on intensity modulated spectroscopy. Niioka *et al.*⁶ examined the function of lower extremity muscles (gastrocnemius in the calf muscle and two muscles in the quadriceps muscle group) during exercise using CW-NIRS. They showed the feasibility of optical imaging for studying muscle function. However, conventional imaging systems do not have a sufficient mapping area; a measurement area of about 10 cm x 10 cm is not sufficient for measurement in the thigh. Moreover, it should be noted that quantitative measurement of tissue oxygenation has not been possible because conventional NIRS is based on the inappropriate assumption that tissues are homogeneous. In muscle oxygenation measurement, the subcutaneous fat layer greatly affects measurement sensitivity⁷⁻¹⁰.

In this study, we developed a 200-channel mapping system for muscle oxygenation that can cover a wide area (30 cm x 20

* Correspondence: E mail: niwa@bme.eng.hokudai.ac.jp; Telephone: +81-11-706-6777; Fax: +81-11-706-7196

cm). This system was applied to measurements of changes in muscle oxygenation in almost the entire region of the thigh during exercise. Furthermore, we applied our correction method^{8,10} for the influence of the fat layer to this mapping system in order to quantitatively image muscle oxygenation.

2. METHODS

2.1. Instrumentation

The developed system has 200 channels and can receive signals from 40 probes, each of which contain 5 channels. As shown in Fig. 1, a probe is composed of a light source, five photo diodes (Hamamatsu Photonics, S2386-18K, 45K), and a current-to-voltage (I-V) converter. A light-emitting diode (OPTRANS, 95010), including two diode-elements of 830- and 770-nm peak wave lengths, was used for the light source. The photo diodes were located at 3 and 15 mm from the light source. A photo diode of 3-mm separation was used to examine the effects of blood within the skin. The photo-diode current was converted to a voltage signal by the I-V converter, which was buried within each probe in order to reduce external noise. In measurement in muscle, an optical probe should appropriately be in contact with the skin surface even when it deforms due to contraction of the muscle. Therefore, the probe was made of silicone so as to fit the skin surface and so that there would be little change in source-detector separation.

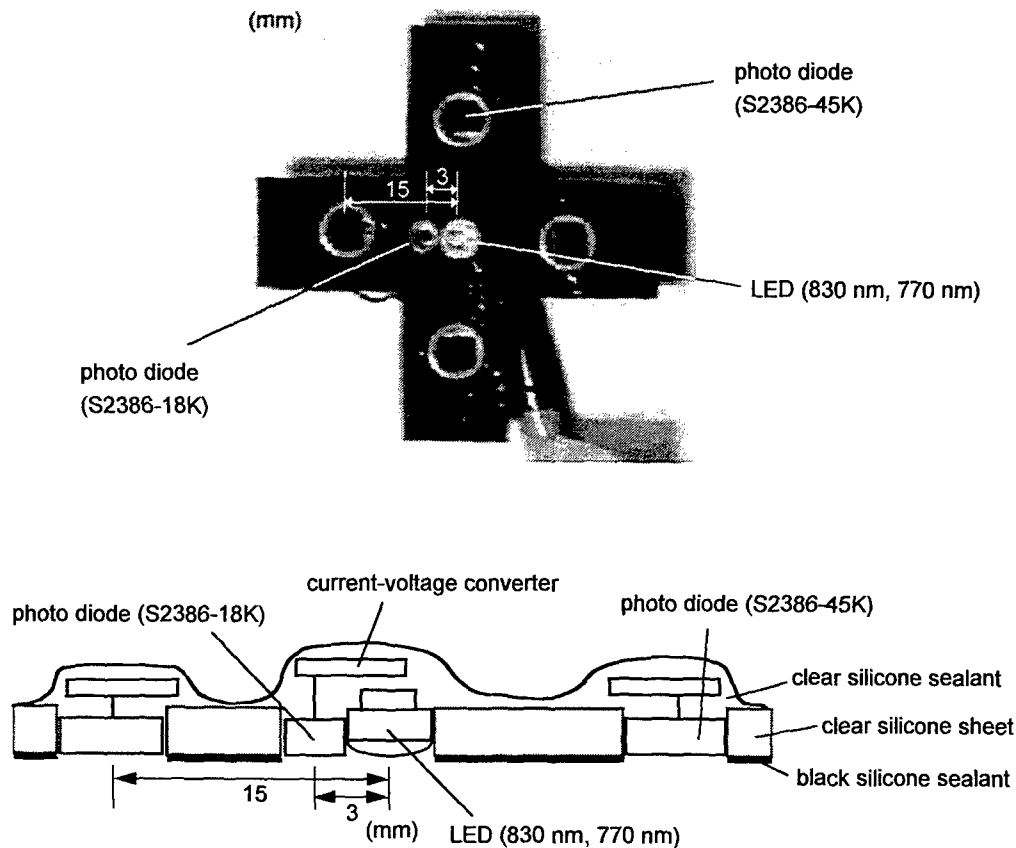


Fig. 1. An optical probe used in the mapping system.

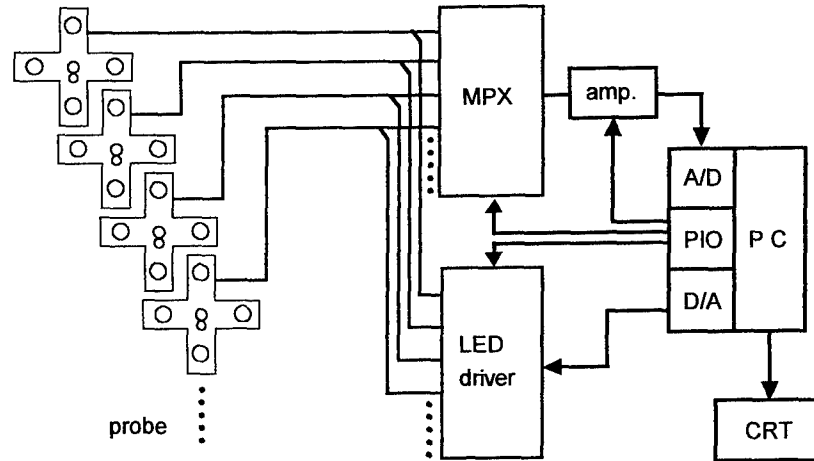


Fig. 2. Block diagram of the mapping system.

A block diagram of the mapping system is shown in Fig. 2. The basic construction is the same as that of oximeters previously reported⁷⁻¹⁰. Voltage outputs from the I-V converter were multiplexed and amplified by 2 to 100 times. The outputs from the amplifier were fed into a personal computer via an A/D converter. The gain of the amplifier and light intensity of the LED were automatically adjusted by the computer in order to obtain an appropriate signal level of detected light at the start of measurement. The data acquisition of 200 channels and calculation of oxygenation were completed within 1.2 s, and traces were displayed on a CRT in real time.

We employed the following equations to determine the change in concentrations of HbO₂, Hb and total Hb.

$$\Delta[\text{HbO}_2] = \frac{1}{\rho \text{DPF}} \frac{\epsilon_{\lambda_2}^{\text{Hb}} \Delta OD_{\lambda_1} - \epsilon_{\lambda_1}^{\text{Hb}} \Delta OD_{\lambda_2}}{\epsilon_{\lambda_1}^{\text{HbO}_2} \epsilon_{\lambda_2}^{\text{Hb}} - \epsilon_{\lambda_2}^{\text{HbO}_2} \epsilon_{\lambda_1}^{\text{Hb}}}, \quad (1)$$

$$\Delta[\text{Hb}] = -\frac{1}{\rho \text{DPF}} \frac{\epsilon_{\lambda_2}^{\text{HbO}_2} \Delta OD_{\lambda_1} - \epsilon_{\lambda_1}^{\text{HbO}_2} \Delta OD_{\lambda_2}}{\epsilon_{\lambda_1}^{\text{HbO}_2} \epsilon_{\lambda_2}^{\text{Hb}} - \epsilon_{\lambda_2}^{\text{HbO}_2} \epsilon_{\lambda_1}^{\text{Hb}}}, \quad (2)$$

$$\Delta[\text{total Hb}] = \Delta[\text{HbO}_2] + \Delta[\text{Hb}], \quad (3)$$

where $\Delta[\text{HbO}_2]$, $\Delta[\text{Hb}]$, and $\Delta[\text{total Hb}]$ are changes in concentrations of HbO₂, Hb, and total Hb, respectively; $\epsilon_{\lambda_{1,2}}^{\text{Hb}}$ and $\epsilon_{\lambda_{1,2}}^{\text{HbO}_2}$ are molar extinction coefficients¹¹ of Hb and HbO₂, respectively, at wavelengths λ_1 and λ_2 ; ρ is source-detector distance; and DPF is a differential pathlength factor¹² based on the assumption that tissue is homogeneous. In this study, DPF was determined by the diffusion theory, the validity of which had been confirmed by our phantom experiments⁹. At a source-detector separation of 15 mm, DPF was 3.1. The changes in concentrations of HbO₂, Hb, and total Hb are expressed as mM.

2.2. Correction of the influence of a fat layer

In order to eliminate the influence of subcutaneous fat layer, we used the correction curve shown in Fig. 3. This curve was obtained from the results of Monte Carlo simulation and the results of two groups of *in vivo* experiments¹⁰. The relationship between normalized measurement sensitivity S and fat layer thickness h was expressed by the following equation:

$$S = \exp\left\{-\left(\frac{h}{A_1}\right)^2\right\} - A_2 G(\alpha, \beta), \quad (4)$$

where $G(\alpha, \beta)$ is a gamma distribution. The constants A_1 , A_2 , α , and β at a source-detector separation of 15 mm were 6.9, 1.15, 7.86 and 0.80, respectively. These constants are dependent on the optical properties of tissues to some extent, but the dependence on the properties is much less than that on fat layer thickness. Thus, the value of S was determined in practice only by h , and then corrected measurements were obtained by dividing the measurements calculated from equations (1)–(3) by S .

Fat thicknesses were measured by a diagnostic ultrasound apparatus (Toshiba, SSA-320A, 7.5-MHz center frequency). The fat layer can readily be distinguished from a muscle layer, because the muscle layer is easily identified by contraction of the muscle. Fat layer thickness was determined by reading the thicknesses on a hard copy of the ultrasound image, as shown in Fig. 4.

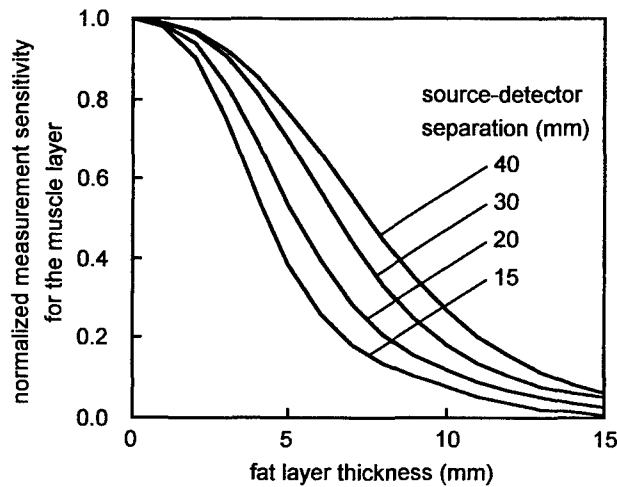


Fig. 3. A curve for correction of the influence of a fat layer: normalized measurement sensitivity for the muscle at each source-detector separation.

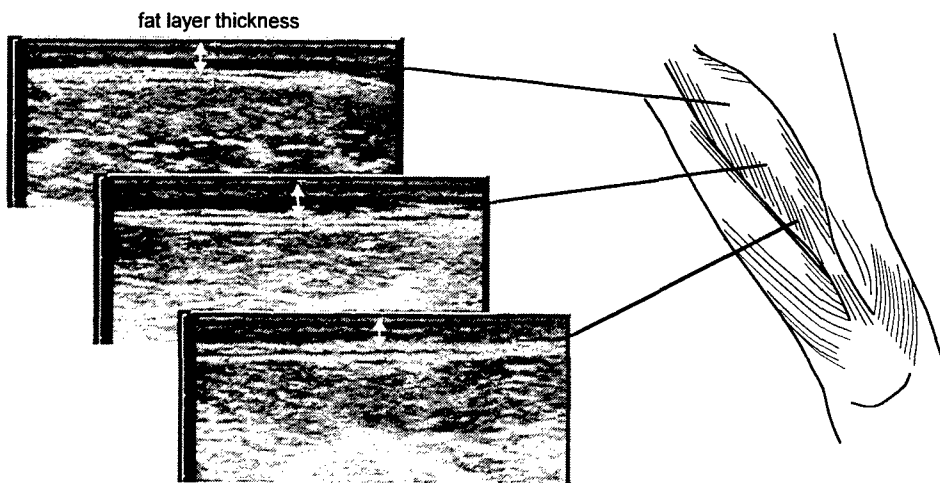


Fig. 4. Thickness of a fat layer measured from an ultrasound image.

2.3. *In vivo* tests

A healthy male (27 years of age and 53 kg in weight) participated in exercise tests. Changes in muscle oxygenation and blood volume were measured in the thigh muscles: vastus lateralis (VL), rectus femoris (RF), vastus medialis (VM), and biceps femoris (BF). The measurement region was 8-23 cm proximal to the center of the patella. We used 28 probes (112 detectors of 15-mm separation and 28 detectors of 3-mm separation) to cover the right thigh. The probes were fixed on the skin surface with surgical tape (3M Health Care, Transpore) at intervals of 5 and 7 cm in circumferential and longitudinal directions, respectively, as shown in Fig. 5. The subject repeated contractions of the maximal isometric knee flexor or extensor for 60 seconds with a 2-minute recovery between the two exercises. Mapping images of 45 cm x 15 cm were obtained.

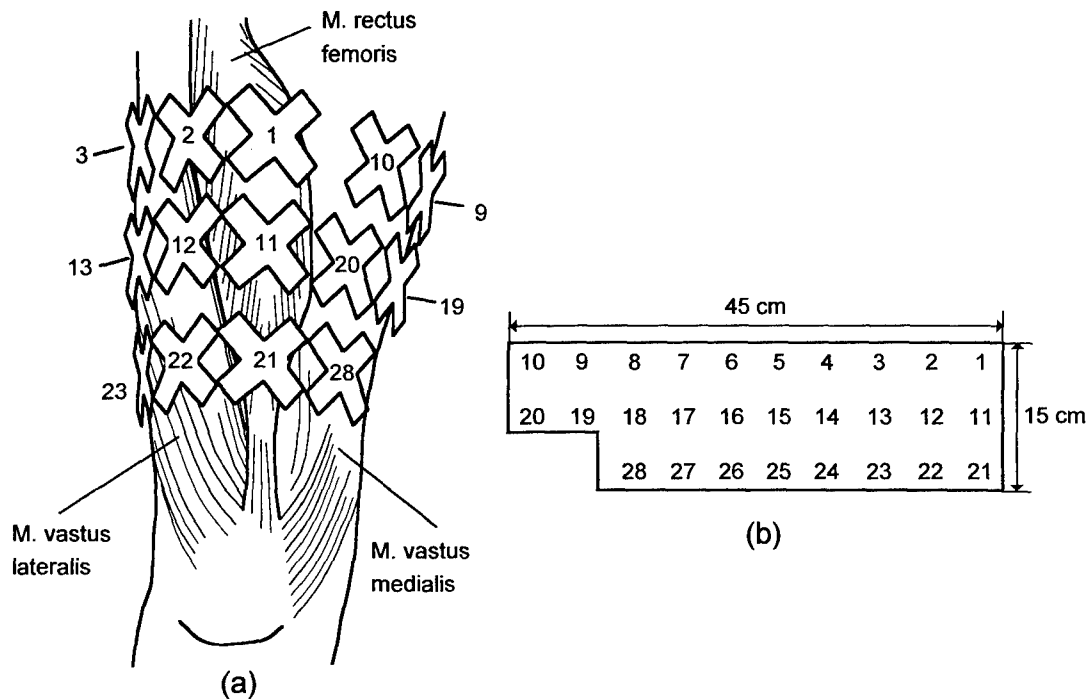


Fig. 5. Arrangement of the parts of the optical probe (a) and arrangement in a mapping image (b).

3. RESULTS AND DISCUSSION

3.1. Mapping of muscle oxygenation

Figure 6 shows an example of traces in each muscle in the exercise test at a source-detector separation of 15 mm. Mapping images were obtained, as shown in Fig. 7. Reduction in blood volume and deoxygenation occurred in the BF muscle during the knee flexion exercise. During recovery, a large hyperemic response was concomitantly found in the medial part of the BF muscle. During knee extension exercise, a marked reduction in blood volume and deoxygenation occurred in the RF and VM muscles. In comparison with these muscles, the VL muscle responded less to the exercise. Thus, the working muscles in the exercises could be imaged, and the heterogeneity of the muscles was successfully shown.

Although the optical probe was designed to be flexible and in contact with the skin surface, signals from some probes placed on a recessed portion were saturated, probably due to direct incidence of light from a source. A more reliable method for fixing optical probes must be used; e.g., light pressure by a flexible cuff wrapped around an array of the probes.

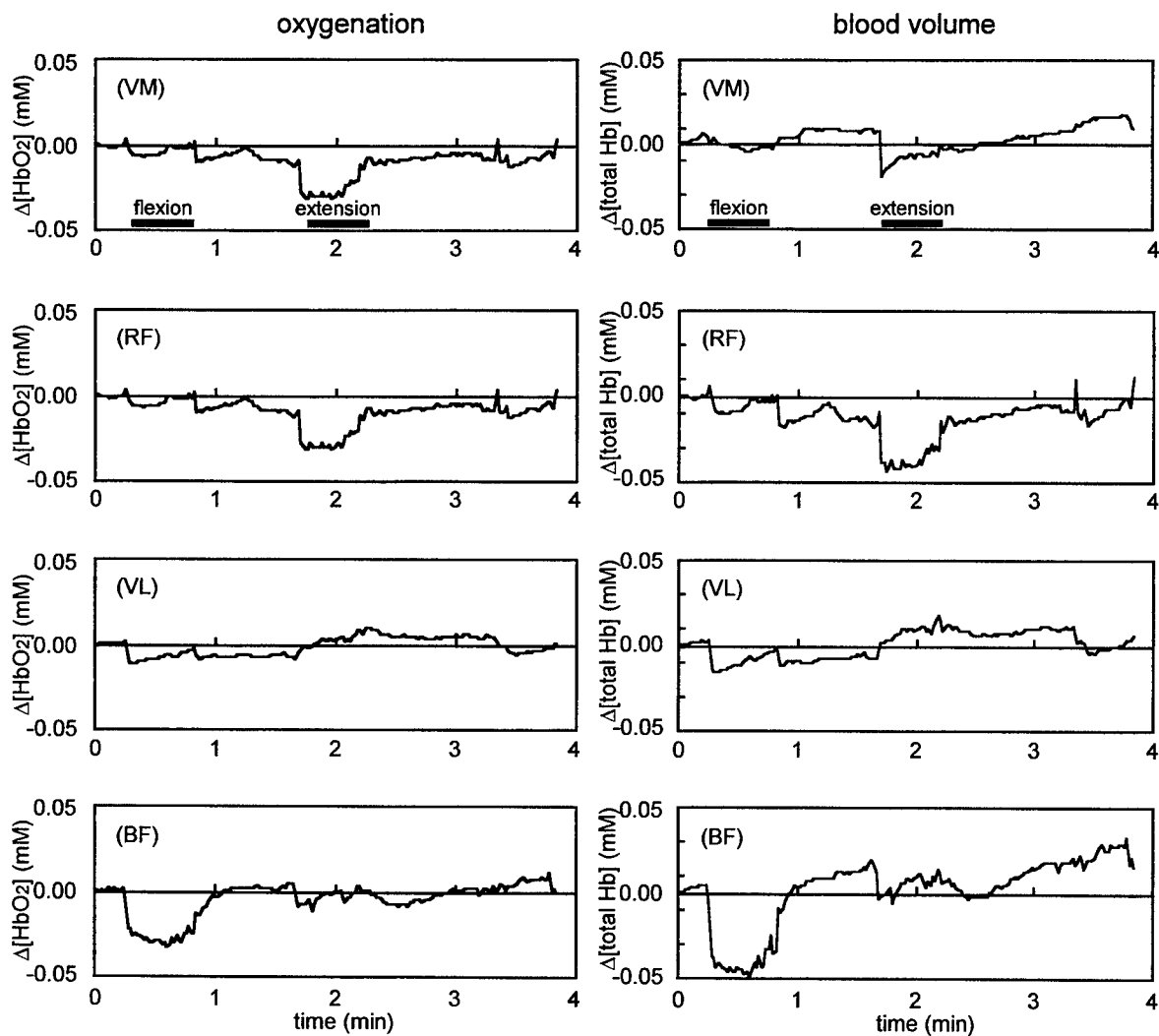


Fig. 6. Typical traces of changes in the concentrations of HbO_2 and total Hb in the thigh muscles: vastus medialis (VM), rectus femoris (RF), vastus lateralis (VL), and biceps femoris (BF). Source-detector separation was 15 mm.

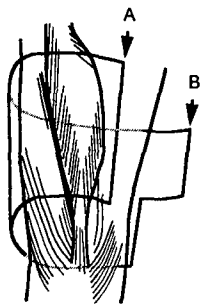
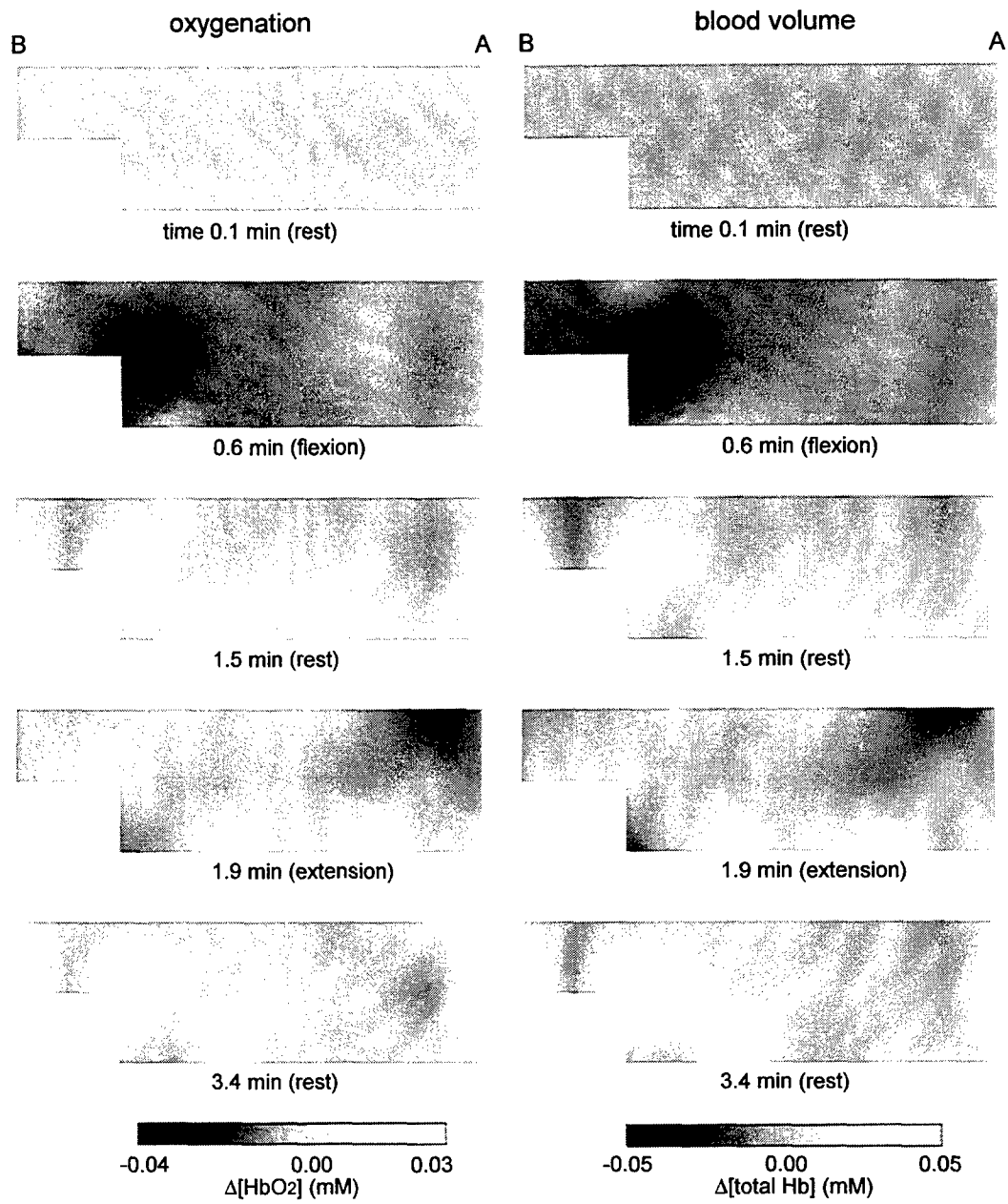


Fig. 7. Mapping images of changes in the concentrations of HbO₂ and total Hb in the thigh.

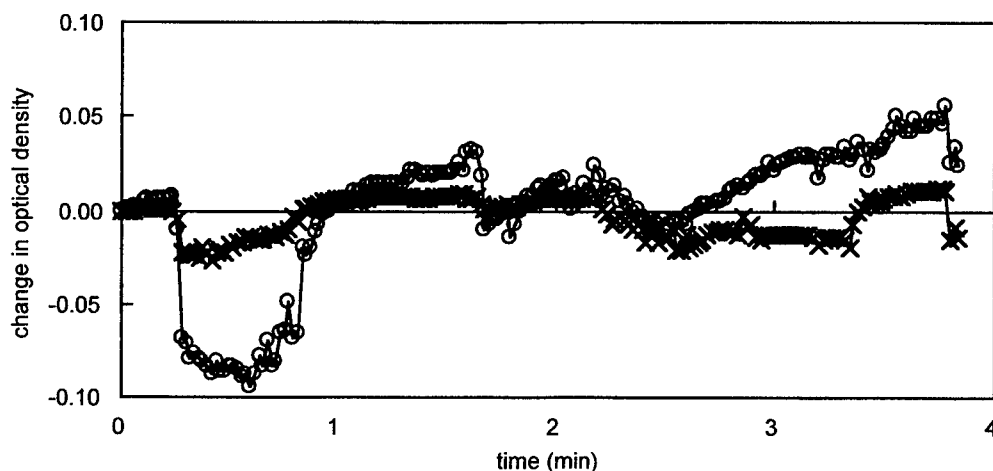


Fig. 8. Changes in optical density at 830 nm obtained at 3-mm (×) and 15-mm separations (○) in the vastus medialis muscle.

3.2. Influence of skin blood flow

The influence of skin blood flow on muscle oxygenation measurement was examined using a detector located at a 3-mm separation from a light source. Figure 8 shows changes in optical density (ΔOD) obtained at source-detector separations of 3 and 15 mm in the VM muscle at a wavelength of 830 nm. The change in optical density of 3-mm separation varied by about 20% of ΔOD of 15-mm separation. This result suggests that there is a significant influence of skin blood flow. This influence could be eliminated by subtracting ΔOD of 3-mm separation from that of 15-mm separation, if measurement sensitivity of 3-mm separation for the muscle can be ignored compared to that of 15-mm separation.

In the experiments, we measured fat layer thicknesses by placing an ultrasound probe on many different portions of the thigh. From a practical point of view, this inefficient procedure should be improved. We have proposed a method for correcting the influence of a fat layer using detected light intensity at rest⁸. This correction method is based on the fact that detected light intensity increases with fat layer thickness due to the much lower absorption of light in a fat layer than in a muscle layer. This relationship can be easily incorporated in a calculation algorithm of an oximeter, although the accuracy of this correction method is not as good as that of the method in the present study, which uses a known measured thickness. Each probe used in the present mapping system also has a near-by detector besides a source for correcting the effects of skin blood flow, as mentioned above. This system enables elimination of both the influences of a fat layer and skin blood flow, and therefore more quantitative and simple measurements can be performed using this system without the need of any additional equipment.

5. CONCLUSIONS

We have developed a 200-channel mapping system using continuous wave near-infrared spectroscopy that covers a wide area and that enables measurement of quantitative changes in oxygenation and blood volume. Mapping images of the entire of the right thigh were able to be obtained using this system, and temporal and spatial heterogeneity of muscle oxygenation during exercise was successfully detected. These results show that the newly developed 200-channel mapping system enables observation of the distribution of muscle metabolism and localization of muscle function.

ACKNOWLEDGMENT

This research was supported in part by Grant-in-Aid for Scientific Research from the Ministry of Education, Science and Culture of Japan.

REFERENCES

1. B. Chance, A. Villringer, V. Dirnagl, and K. M. Einhaupl, "Optical imaging of brain function and metabolism," *J. Neurology*, **239**, pp. 359-360, 1992.
2. A. Maki, Y. Yamashita, Y. Ito, E. Watanabe, Y. Mayanagi, and H. Koizumi, "Spatial and temporal analysis of human motor activity using noninvasive NIR topography," *Med. Phys.*, **22**, pp. 1997-2005, 1995.
3. J. R. Mansfield, M. G. Sowa, and H. Mantsch : "Near-infrared spectroscopic reflectance imaging : methods for functional imaging and in vivo monitoring," *Proc. SPIE*, **3597**, 270-280, 1999.
4. Y. Chen, S. Zhou, S. Nioka, and B. Chance, "A Novel Portable System for Neonatal Brain Imaging," *Proc. SPIE*, **3597**, 262-269, 1999.
5. M. Maris, E. Gratton, J. Maier, W. Mantulin, and B. Chance, "Functional near-infrared imaging of deoxygenated hemoglobin during exercise of the finger extensor muscles using the frequency-domain technique," *Bioimaging*, **2**, pp. 174-183, 1994.
6. S. Nioka, H. Miura, H. Long, A. Perry, D. Moser, and B. Chance: "Functional muscle imaging in elite and untrained subjects", *Proc. SPIE*, **3597**, 282-290, 1999.
7. K. Yamamoto, M. Niwayama, T. Shiga, L. Lin, N. Kudo, and M. Takahashi, "Accurate NIRS measurement of muscle oxygenation by correcting the influence of a subcutaneous fat layer," *Proc. SPIE*, **3194**, pp. 166-173 1998.
8. K. Yamamoto, M. Niwayama, T. Shiga, L. Lin, N. Kudo, and M. Takahashi, "A near-infrared muscle oximeter that can correct the influence of a subcutaneous fat layer," *Proc. SPIE*, **3257**, pp. 145-155, 1998.
9. L. Lin, M. Niwayama, T. Shiga, N. Kudo, M. Takahashi, and K. Yamamoto, "Two-layered phantom experiments for characterizing the influence of a fat layer on measurement of muscle oxygenation using NIRS," *Proc. SPIE*, **3257**, pp. 156-166, 1998.
10. M. Niwayama, L. Lin, J. Shao, T. Shiga, N. Kudo, and K. Yamamoto, "Quantitative measurement of muscle oxygenation by NIRS: Analysis of the influences of a subcutaneous fat layer and skin," *Proc. SPIE*, **3597**, pp. 291-299, 1999
11. S. J. Matcher, C. E. Elwell, C. E. Cooper, M. Cope, and D. T. Delpy, "Performance comparison of several published tissue near-infrared spectroscopy algorithms," *Analytical Biochemistry*, **227**, pp. 54-68, 1995.
12. D. T. Delpy, M. Cope, P. van der Zee, S. Arridge, S. Wray, and J. Wyatt, "Estimation of optical pathlength through tissue from direct time of flight measurement," *Phys. Med. Biol.*, **33**, pp. 1433-1442 (1988).